CHEMISTRY
A EUROPEAN JOURNAL

DOI: 10.1002/chem.200801602

Gated and Differently Functionalized (New) Porous Capsules Direct Encapsulates' Structures: Higher and Lower Density Water

Tamoghna Mitra,[a] Pere Miró,[b] Adrian-Raul Tomsa,[a] Alice Merca,[a] Hartmut Bögge,[a] Josep Bonet Ávalos,[c] Josep Maria Poblet,[d] Carles Bo,*[b, d] and Achim Müller*[a]

Dedicated to Professor Bernt Krebs on the occasion of his 70th birthday

Abstract: By the deliberate choice of the internal ligands of the porous nanocapsules $[\{(Mo)Mo_5\}_{12}\{Mo_2(ligand)\}_{30}]^{n-}$, the respective cavities' shells can be differently sized/functionalized. This allows one to trap the same large number of water molecules, that is, 100 in a capsule cavity with formate ligands having a larger space available, as well as in a cavity containing sulfates and hypophosphites, that is, with less space. Whereas the 100 molecules fill the space completely in the second case in which they are organized in three shells, a four-shell system with underoccupation and broken hydrogen bonds is observed in the other case. This is an unprecedented result in terms of the structurally well defined special forms of "higher and lower density" water molecule assemblies. Precisely, by replacing the larger ligands in the mentioned nanocapsule type by formates, voids in the capsule cavity of $(HC(NH_2)_2)_{22}[\{(HC(NH_2)_2)_{20}+(H_2O)_{100}\}\subset\{(Mo)Mo_5O_{21}(H_2O)_6\}_{12}\{Mo_2O_4(HCO_2)\}_{30}]\cdot ca.\,200\,H_2O$ are generated that get filled with water molecules concomitant with an expansion of the three to four shell $\{H_2O\}_{100}$ cluster. The water shells in both capsules containing different ligands are organized in the form of dodecahedra (partly with underoccupation) and a strongly distorted rhombicosidodecahedron spanned by a $\{H_2O\}_{60}=\{(H_2O)_5\}_{12}$ aggregate. The well-defined water shells only emerge if cations cannot enter into the capsules, which is achieved by closing the pores with plugs/guests such as formamidinium cations. The work is based on the syntheses of two new compounds, related single-crystal X-ray diffraction studies, and molecular dynamics simulations, which show remarkably that water molecule shell structuring occurs in the capsules due to the confined conditions even in the case of open pores and at room temperature if cation uptake is prevented.

Keywords: capsules · confinement · nanostructures · polyoxometalates · self-assembly · water structures

[a] T. Mitra, Dr. A.-R. Tomsa, Dr. A. Merca, Dr. H. Bögge, Prof. Dr. A. Müller
Fakultät für Chemie der Universität
Postfach 100131, 33501 Bielefeld (Germany)
Fax: (+49) 521-106-6003
E-mail: a.mueller@uni-bielefeld.de

[b] P. Miró, Prof. Dr. C. Bo
Institute of Chemical Research of Catalonia (ICIQ)
Avinguda dels Països Catalans 16
43007 Tarragona (Spain)
E-mail: cbo@iciq.es

[c] J. B. Ávalos
Departament d'Enginyeria Química
ETSEQ
Universitat Rovira i Virgili
Avinguda dels Països Catalans 26
43007 Tarragona (Spain)

[d] Prof. Dr. J. M. Poblet, Prof. Dr. C. Bo
Departament de Química Física i Inorgànica
Universitat Rovira i Virgili
Avinguda Marcelli Domingo s/n
43007 Tarragona (Spain)

Supporting information for this article is available on the WWW under http://dx.doi.org/10.1002/chem.200801602.

Introduction

Chemical studies based on confined conditions involve interesting interdisciplinary aspects.[1] The use of nanosized carbon tubes[2]or metal oxide based capsules (as in the present investigation) has advantages as it allows one to work under a variety of experimental conditions. In this context encapsulated water molecule assemblies are of special interest because they are of relevance for several aspects of molecular biology, for example, protein folding and activity.[3,4] Regarding the problem of understanding the structure of bulk liquid water[5–7] so-called two-structure models were developed[7a,j–l] (see also reference [3d]), while with reference to biological scenarios it is assumed in the literature that the liquid consists of rapidly exchanging high density water (HDW) and low density water (LDW) microdomains differing in their physical and chemical properties because of their different strength of hydrogen bonds;[8,9] a corresponding paper related to biological aspects is entitled "Life depends upon two kinds of water".[9] In this context we can read: "[…] protein conformations demanding greater hydration are favored by more (re-)active water (for example, high density water containing many weak bent and/or broken hydrogen bonds) and 'drier' conformations are relatively favored by lower activity water (for example, low-density water containing many strong intra-molecular aqueous hydrogen bonds)".[9b] In any case it is generally accepted that networks of hydrogen-bonded water assemblies (especially the "high density" ones!) control protein folding, structures, and activities; see for instance reference [4b].

In recent years the effect of confinement on properties of "materials" has been investigated including general aspects,[10] but of course also considering liquids[11] and these especially in context with confined water properties.[12–15] One possible way to investigate confined water molecule assemblies systematically is by trapping them in structurally well defined and differently sized as well as functionalized nanosized capsule cavities. This is possible with soluble spherical porous capsules of the type $[\{\text{pentagonal unit}\}_{12}\{\text{metal linker unit}\}_{30}]^{n-} \equiv [\{(Mo^{VI})Mo^{VI}{}_5O_{21}(H_2O)_6\}_{12}\{Mo^{V}{}_2O_4(\text{ligand})\}_{30}]^{n-}$,[16a,b] which are stable in solution under well-defined conditions, while the pores can, as an important aspect, be closed in a stepwise manner.[16c] (They have—because of their properties—been described as artificial cells.[16d]) These capsules, which can be considered as coordination polymers with spherical periodicity—the pentagonal units acting as ligands[16e]—can be constructed with differently sized cavities based on the choice of internal ligands. After it was possible to fill completely the cavity of a $\{Mo_{132}\}$-type capsule containing SO_4^{2-} and $H_2PO_2^-$ ligands with 100 water molecules,[16f,g] it was a challenge to study the water assembly in a capsule cavity with enlarged space. This could now be achieved by the incorporation of the smallest appropriate bidentate ligands, namely formates. (The related types of compounds are accessible by facile syntheses[16h] and their properties are now studied by many groups.[16i]) The fact that in this context structurally well-defined "higher and lower density" forms of water molecule assemblies can be studied seems to show the route for further investigations. The obtained experimental results can be compared with information obtained from computational studies. After molecular dynamics simulations were applied recently for the study of water encapsulated in nanotubes,[17] in reverse micelles,[18] and that confined in nanospaces between solid layers,[19] we applied these well-established computational methods now for the present cases.

Results and Discussion

Syntheses and structures: Compound **1**, which contains the $\{Mo_{132}\}$-type capsules with the largest possible cavity, was prepared by replacing acetate ligands[16a,b,h] in the corresponding compound by formates[20] (for the formula of the starting material see the Experimental Section). Compound **1** was characterized analytically, spectroscopically (IR, Raman), and by complete single-crystal X-ray structure analysis (see Table 1 and the Experimental Section). The

Table 1. Crystallographic data for **1**, **2**, and **3**

Compound	**1**	**2**	**3**
formula	$C_{30}H_{1002}Mo_{132}N_{42}O_{834}$	$C_{72}H_{984}Mo_{132}N_{84}O_{804}$	$C_{216}H_{3576}Mo_{528}N_{648}O_{2892}P_{72}S_{48}$
crystal size [mm]	$0.30\times0.30\times0.22$	$0.40\times0.40\times0.20$	$0.30\times0.20\times0.20$
Fw [g mol^{-1}]	27966.8	28561.5	115970.9
space group	$R\bar{3}$	$R\bar{3}$	$R\bar{3}m$
a [Å]	32.6385(13)	32.7062(11)	62.865(2)
c [Å]	73.416(4)	74.393(4)	76.470(4)
V [Å^3]	67730(5)	68917(5)	261720(13)
Z	3	3	3
T [K]	188(2)	183(2)	188(2)
F (000)	41076	41940	169704
ρ_{calcd} [g cm^{-3}]	2.057	2.065	2.207
$\mu(Mo_{K\alpha})$ [mm^{-1}]	1.882	1.851	2.01
reflections collected	133931	114231	454502
Θ range	$(1.82<\Theta<26.99°)$	$(1.81<\Theta<26.98°)$	$(0.65<\Theta<25.03°)$
unique reflections	32721	32149	52923
obs. refl. ($I>2\sigma(I)$)	25404	23769	35303
R(int)	0.0363	0.0388	0.0911
$R1$[a]($I>2\sigma(I)$)/$R1$(all reflections)	0.0491/0.0709	0.0569/0.0867	0.0820/0.1381
$wR2$[b]($I>2\sigma(I)$)	0.1303	0.1441	0.1884
GooF[c]	1.107	1.145	1.158
max/min residual electron density [e Å^{-3}]	2.045/−1.107	1.727/−0.906	3.336/−2.227

[a] $R1=\Sigma||F_0|-|F_c||/\Sigma|F_0|$. [b] $wR2=[\Sigma[w(F_0^2-F_c^2)^2]/\Sigma[w(F_0)^2]]^{0.5}$ where $w=1/\sigma^2(F_0^2)+(aP)^2+bP$, $P=(F_0^2+2F_c^2)/3$. [c] $GooF=[\Sigma[w(F_0^2-F_c^2)^2]/(n-p)]^{0.5}$.

anionic capsule **1a** contains, as that of the starting material with acetate ligands,[16a,b,g] 12 pentagonal units $\{(Mo)Mo_5O_{21}(H_2O)_6\}^{6-}$ placed at the 12 vertices of an icosahedron and linked by 30 dinuclear $\{Mo^{V}_2O_4(HCO_2)\}^{+}$ units. The construction principle automatically leads to capsules with 20 $\{Mo_9O_9\}$ pores[16f] (see Figure 1, top-left). As these have crown ether function they can all be closed with complementary guests/plugs like formamidinium cations in agreement with the principles of supramolecular chemistry.[16d,f] (This allows one to prepare compound **2** with closed capsule pores as mentioned below.) The interior of the cavity of **1a** should be briefly discussed; see also the Conclusions and Outlook. It hosts a well-defined water $\{H_2O\}_{80}$ cluster consisting of a $\{H_2O\}_{60}$ shell that is embedded into a peripheral dodecahedral $\{H_2O\}_{20}$ shell (Figure 1, top right), while the two shells interact via hydrogen bonds. (The $\{H_2O\}_{80}$ is also found in the corresponding $\{Mo_{132}\}$-type capsule with $H_2P_2O_2^-$ ligands.[16g]) However the cavity of **1a** should not be completely free of NH_4^+ ions (see formula), since the 20 pores remained open during the synthesis with the consequence that this influences the structure of the disordered encapsulate $\{nNH_4^+ + mH_2O\}$ in the central part of the cavity; for the related problem of positioning crystallographically NH_4^+ ions disordered with H_2O molecules, see below. The complete encapsulate can in principle be considered as a nanosized water-electrolyte assembly (see ref. [16g]).

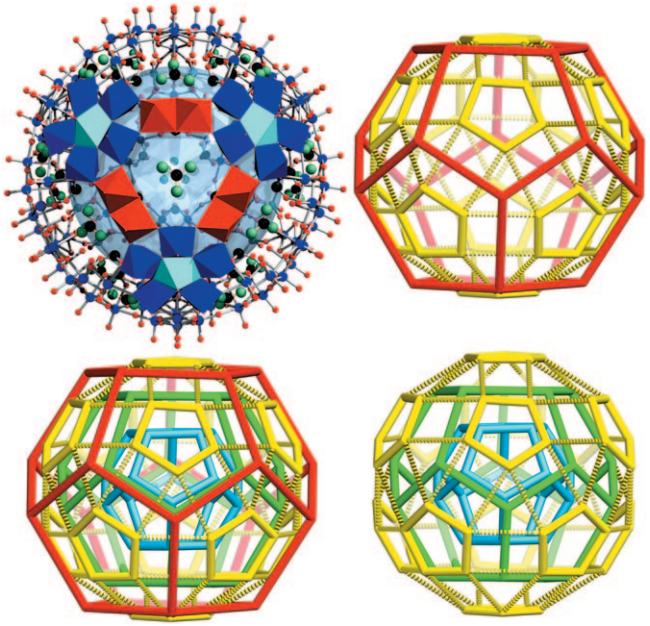

Figure 1. Structure of the different water molecule assemblies (in wireframe representation showing only the O atoms) occurring within the cavities of the three different spherical porous $\{Mo_{132}\}$-type polyoxomolybdates **1a**, **2a**, and **3a**, while hydrogen bonds between the shells are not shown. Top right: Scenario in open **1a** showing the peripheral $\{H_2O\}_{20}$ (red) and the inner $\{H_2O\}_{60}$ shell, while highlighting the 12 $(H_2O)_5$ pentagons (yellow, like for **2a** and **3a**). Bottom left: The situation in **2a** (underoccupation not shown) showing the three dodecahedra, that is, one fully occupied (light blue) and the two underoccupied $\{H_2O\}_{20/2}$ types (red and green), as well as the $(H_2O)_{60}$ shell (yellow). Bottom right: Shown is the three-shell water assembly in **3a** on the crystallographic site 2/*m*; the central (blue) and the peripheral (yellow) shells correspond to those in **2a**. Additionally shown (top left) is the structure of the present capsule type, that is, that of **2a** highlighting one pore (in polyhedral representation with the pentagonal units in blue and dinuclear linkers in red) and showing the noncovalently bonded formamidinium cations/plugs (C black, N/H green; because of the disorder a threefold axis in the central pore is visible). The small formate ligands lying below the dinuclear linkers are difficult to identify. The large blue sphere highlights the cavity in which the water molecules are encapsulated (remaining color codes for the atoms of the ball-and-stick part: Mo blue, O red).

$$(NH_4)_{42-n}\ [\{(NH_4)_n+(H_2O)_{80+m}\} \subset \{(Mo)Mo_5O_{21}(H_2O)_6\}_{12}\{Mo_2O_4(HCO_2)\}_{30}]$$
$$\cdot \text{ca. } 250H_2O \equiv (NH_4)_{42-n} \cdot \mathbf{1a} \cdot \text{ca. } 250\,H_2O \equiv \mathbf{1}^{[21]}$$

To study the nature of a pure encapsulated water molecule assembly in the cavity of **1a**, that is, in the absence of inorganic cations[22] (these would decrease the number of uptaken water molecules) compound **2** was prepared from **1** by replacing the ammonium by formamidinium cations (see Experimental Section). Compound **2** was characterized with the same methods as **1**; see above as well as the Experimental Section and Table 1. Compound **2a** has the same skeleton as **1a** but closed pores due to the presence of the new cations. Formamidinium cations are too large to pass through the 20 $\{Mo_9O_9\}$ pores/gates but can close them as mentioned above (see Figure 1, top left). The new scenario shows as expected a cation-free water cluster integrated in the capsule cavity. As regards pore closing it should be mentioned that in solutions of compounds such as **2**, the affinity of the capsule pores to cationic plugs depends strongly on the type of solvent or solvent mixture.[16d] In organic solvent–water mixtures the tendency for complete closure decreases with increasing concentration of H_2O. On the other hand the precipitation of compounds such as **2** from aqueous solution in water in the form of salts is favored, as pore closing with the positively charged plugs (present in excess) leads to a decrease of the anionic charges of the capsules and therefore to a decrease of the solubility.[16d]

$$(HC(NH_2)_2)_{22}\ [\{(HC(NH_2)_2)_{20}+(H_2O)_{100}\}$$
$$\subset \{(Mo)Mo_5O_{21}(H_2O)_6\}_{12}\{Mo_2O_4(HCO_2)\}_{30}]$$
$$\cdot \text{ca. } 200\,H_2O \equiv (HC(NH_2)_2)_{22} \cdot \mathbf{2a}$$
$$\cdot \text{ca. } 200\,H_2O \equiv \mathbf{2} \text{ (see Table 1)}$$

The encapsulated water molecules in **2a** are found arranged in a well-defined and unprecedented structure that can be described by a four concentric shell arrangement with radii of 3.92–4.13, 6.72–6.78, 7.59–7.78, and 8.31–8.70 Å. The shells have the following composition/structures in the same sequence: $\{H_2O\}_{20}$/dodecahedral, $\{H_2O\}_{20/2}$/dodecahedral type, $\{H_2O\}_{60}$/distorted rhombicosidodecahedral, and $\{H_2O\}_{20/2}$/dodecahedral type (Figure 1 and Figure 2), while the two $\{H_2O\}_{20/2}$ shells are not separated enough from each other (related O···O distances on the C_3 axes <2 Å) to allow a complete occupation. As a consequence of this, the

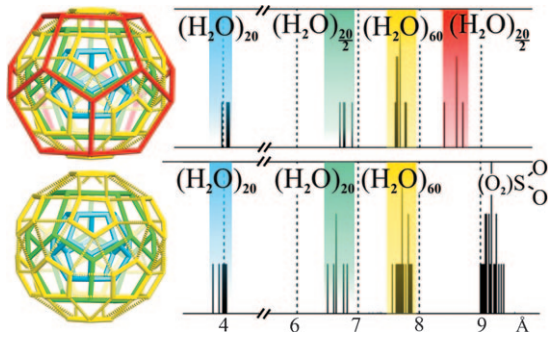

Figure 2. The distance histograms related to capsules **2a** (top) and **3a** (bottom): Shown are the distributions of oxygen atoms of the water molecules at the different distances from the center of the cavities. Compound **3a** lacks, because of the large sulfates (see text), enough space to place the 4th shell present in **2a** (color code as in Figure 1). (The distances to the terminal O atoms of the sulfate ligands are given for **3a**, too.)

water molecules are distributed statistically at the vertices of the two dodecahedra, while both show occupancies of 50%. If a H_2O molecule occurs in one of the two dodecahedra the position of the second dodecahedron on the same C_3 axis is vacant.

Remarkably, the same number of 100 water molecules as in **2a** was also found in the earlier published capsule anion **3a**, the cavity of which is completely filled[16f,23] (see also Experimental Section and Table 1 with the whole formula of **3**[23]). But in that case three concentric fully occupied shells—interacting via hydrogen bonds -are present, which are organized in the form of two $\{H_2O\}_{20}$ dodecahedra and one strongly distorted $\{H_2O\}_{60}=\{(H_2O)_5\}_{12}$ rhombicosidodecahedron (radii of the shells are 3.84–4.04, 6.51–6.83, and 7.56–7.88 Å, respectively; see Figure 1 and 2 showing the basic $\{H_2O\}_{100}$ structure with approximate icosahedral symmetry).

$$[\{(C(NH_2)_3)_{20}+(H_2O)_{100}\}\subset\{(Mo)Mo_5O_{21}(H_2O)_6\}_{12}\{Mo_2O_4(H_2PO_2)\}_{20}\{Mo_2O_4(SO_4)\}_{10}]^{32-}$$ **3a**[16f,22]

The important comparison of **2a** and **3a**[16f,23] reveals that the larger ligands, $H_2PO_2^-$ and SO_4^{2-}, of **3a** block the available space in the internal cavity relatively to that of **2a**, which contains formate ligands. The difference is (mostly) responsible for the different structures of the two $\{H_2O\}_{100}$ assemblies, a result which will be discussed in the section Conclusions and Outlook, too. This scenario can be described as "high and low density" water molecule assemblies, while the terms HDW/LDW are considered relative(!) to each other, that is, related to the present system and not in a general consideration! Important in this context is that the present "low density" case shows more broken hydrogen bonds, which is reverse to the bulk scenario (discussed in the Introduction).

Molecular dynamics simulations: To gain more insight into the nature and formation of the water assemblies, as well as the uptake of cations at room temperature, a series of classical molecular dynamics simulations (see Experimental Section) on models of **1a**, **2a**, and **3a** (with only 30 sulfate and no hypophosphite ligands) in water as solvent were carried out. Our goal was to investigate computationally different configurations of water clusters inside the different capsules, and to get hints about whether water molecules inside the capsules self-assemble spontaneously or not. In these sort of "numerical experiments", starting from a randomly generated configuration, solvent water molecules and counterions (Na^+ in the case of **1a** and **3a**, and guanidinium cations in the case of **2a**) were allowed to diffuse freely in the simulation box, while the geometry of the capsule including that of the normally flexible ligands was kept frozen. Assumed capsule rigidity causes the channel diameters to be too small to allow the entrance of (hydrated) Na^+ into capsule **3a**, in contrast to the situation for the real **3a** in solution.[16d] Thus, in our simulations **3a** behaves in that respect as a closed capsule. However, when the sulfate ligands were (formally) substituted by formate ligands, that is, referring to **1a**, the related enlarged channels allowed Na^+ ions to pass through. Therefore, plugs had to be present in **2a** to avoid cation uptake. Initially, counterions were distributed around the capsule, which was filled and surrounded by water. Following a standard protocol, a large number of configurations (see the Supporting Information) were collected and analyzed. Then, the radial (RDF) and spatial (SDF) distribution functions of the centers of the capsule-oxygen water atoms were computed.

For capsule **3a** the computed RDFs showed three significant peaks (besides a shallow inner peak not counted in Table 2), signalling a three-shell structure. An agreement of the main features with the experimentally determined distances between the capsule center and the capsule–water oxygen atoms was found. As Figure 3 (top) and Table 2 show, the three main peaks in the RDF were located at 4.4, 6.7, and 7.4 Å. This result means that although during the simulations water molecules can diffuse inside the capsule continuously, a layered shell type structure is obtained caused by the ("templating") confinement. In other words the dynamic structure matches the static experimental data reasonably well. However, note that the calculation of the number of water molecules in each shell, which were computed by integrating the radial distribution function, $g(r)$, can only be approximate (see Figure 3, top).

When the space distribution function was plotted it revealed a clear polyhedral-type structure. The highest proba-

Table 2. Experimental versus computed distances from the center of the capsule to oxygen atoms of water molecules. All values are given in Å (the peaks related to the capsule centers are not considered).

	3a		**2a**	
	experimental	calculated	experimental	calculated
Peak 1	3.84–4.04	4.4	4.02–4.08	4.4
Peak 2	6.51–6.83	6.7	6.62–6.72	6.9
Peak 3	7.56–7.88	7.4	7.66–7.78	7.9
Peak 4	–	–	8.52–8.79	8.8

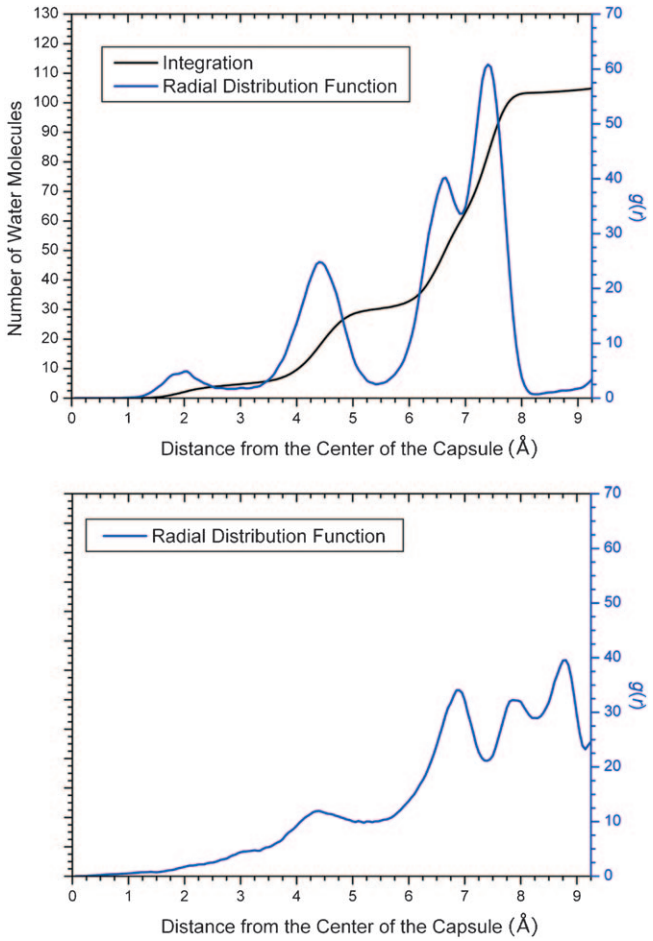

Figure 3. Radial distribution functions (blue lines) showing the distribution of water oxygen atoms from the center of the capsule for different water assemblies formed within the cavities of **3a** (top; the peak at ca. 2 Å corresponds to a small number of water molecules in the capsule center) and **2a** (bottom). Each peak describes the most probable location of water molecules. The number of water molecules obtained by integration of the peak areas are only referred to in the top figure (see text).

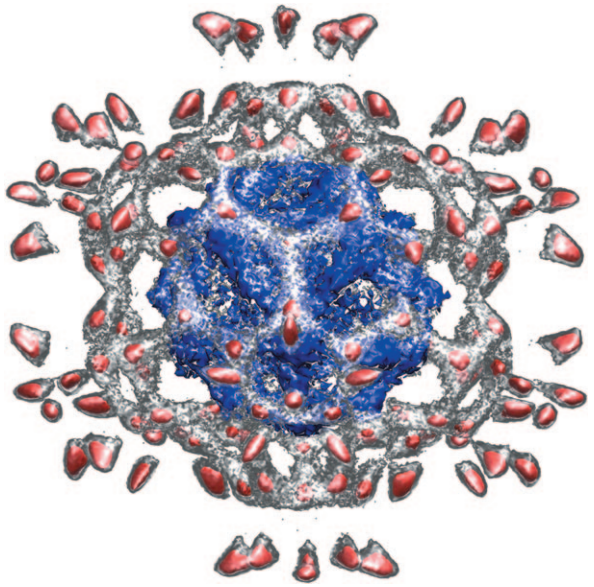

Figure 4. Isosurfaces of the spatial distribution function (SDF) for water oxygen atoms inside capsule **3a**. Two isosurfaces are shown: one colored red and the other colored either gray-transparent or blue, for clarity. The red isosurface corresponds to the regions of maximum probability of finding water oxygen atoms. We found 152 red nodes, which are located precisely at the same positions that we found in the X-ray structure: the dodecahedral second layer (20), the distorted rhombicosidodecahedron third layer (60), and the twelve centered-pentagons of the coordinated water molecules (72). The gray-transparent isosurface corresponds to a probability one order of magnitude lower than the red isosurface, and indicates exchange between the second and third layer. The blue isosurface (same SDF value as the gray one) shows the inner shell.

bility regions of finding water molecules inside the capsule (red areas in Figure 4) correspond to water ligands coordinated to the metal atoms of the 12 $\{(Mo)Mo_5\}$ moieties, that is, to the 12 $\{(H_2O)(H_2O)_5\}$ type pentagons. These ligand-type water molecules remain, as expected, fixed at their locations of maximum probability. (The related shell, located at about 10 Å from the center of the capsule, is not shown in the RDF profile in Figure 3.) The two shells at 7.4 and 6.7 Å (Table 2 and Figure 3) form the same polyhedra as were found crystallographically, that is, a strongly distorted $\{H_2O\}_{60} \equiv \{(H_2O)_5\}_{12}$ rhombicosidodecahedron and a $\{H_2O\}_{20}$ dodecahedron. In these nodes, the grey isosurface extends towards the edges that connect the vertices of the polyhedra, thus suggesting that water molecules in these shells are rather mobile and can exchange their locations. The exchange seems to occur through the edges and not through the faces of the polyhedra. This phenomenon was of course not observed in the crystals since they were measured at low temperatures. Visual inspection of the trajectories indicates a stepwise motion with molecules frequently switching between the shells and in a synchronous way, like a *dynamical hydrogen-bonded gear*. The result corresponds especially to the non-negligible overlap between the peaks at 6.7 and 7.4 Å in the RDF in Figure 3, top. Furthermore, the blue isosurface depicted in Figure 4 (peak at 4.4 Å in Figure 3) is not connected with the second and third shells, as a result of the zero overlap between the corresponding peaks in the RDF. In this inner layer, water molecules are much more mobile than those in the two outer layers, and consequently, no regions of high probability (red regions in Figure 4) are found. Although water behaves more liquid-like in this inner part, the polyhedral shape of the SDF blue isosurface suggests a constrained motion imposed by the symmetry of the capsule.

When a model for **2a** was considered, the RDF plot, as shown in Figure 3 (bottom), displayed a rather different behavior. Instead of the three main peaks found for **3a** a fourth peak appeared at 8.8 Å, in agreement with the experiment (see Table 2). But the additional space available inside the capsule allowed water molecules to be more mobile, and consequently, the RDF peaks strongly overlap. In this case, integration of the peaks is not straightforward. Contrary to the case of **3a**, the SDF function for **2a** did not reveal any clear image since the diffusion during the simulation was rather high due to the large pores (Figure 5) not

closed by guanidinium cations under the present conditions (water as solvent and the comparably low charged capsule) and the occurrence of the formate ligands.

To summarize: In the case of **2a** and **3a**, our simulations showed that encapsulated water molecules self-assemble dynamically in shell structures, which are strongly affected by (slightly) increasing the volume of the capsule. In the case of **2a**, the calculations were done in the presence of guanidinium cations, which close the pores to prevent the uptake of small cations.

To simulate correspondingly the behavior of capsule **1a**, we ran a simulation in the presence of 42 Na^+ ions while leaving the pores open. (Na^+ ions were used in the simulations as they are easily taken up because of their size and the large pores (Figure 5). This allows us to nicely investigate how this affects the encapsulated water structure.) In this case, three cations were detected inside the capsule at the end of the trajectory. The presence of the cations strongly affected the structure of the encapsulated water locally, that is, the shell structure was partly disrupted, although its reminiscence was still observed (see the Supporting Information). Therefore, these results support the scenarios found based on several related single-crystal X-ray studies (see above); small variations in the composition of the capsule and/or the presence of cations being able to enter through the pores, alter significantly the structures of the encapsulated water assemblies.

Conclusions and Outlook

We have investigated two porous spherical $\{pentagon\}_{12}$-$\{linker\}_{30}$-type capsules having different space available for encapsulates in their cavities. The capsules can, for instance, host, in the absence of small inorganic cations, a maximum number of 100 water molecules. This allows us to refer to "higher and lower density" water molecule assemblies as the same number of molecules can be trapped in the two capsule scenarios; the three-shell $\{H_2O\}_{100}$ water cluster of **3a** expands to a four-shell type with underoccupation in the cavity of **2a**. These observations, based on single-crystal X-ray diffraction data, are in reasonable agreement with those from our molecular simulations referring mostly to **3a**. Furthermore, the related spatial distribution function—obtained at room temperature!—reflects the selective mobility of the water molecules confined in the cavities, that is, not all water molecules exhibit the same dynamical behavior. It was also found in this context that the water molecule shells lying close to the internal capsule surface where the important template functions of the coordinated water ligands act (see, for example, ref. [25]) are (highly) ordered, that is, in contrast to the molecules in the central part of the capsule.

The present capsules can—generally speaking—function as templates for "materials" fabrication, for instance, to construct different structurally well-defined types of water cluster aggregates (but not only these[24b]) with and without broken hydrogen bonds. In the latter situation—also called the "tetrahedral type of water" (tetrahedral four-donor motif[3d])—each water molecule is bonded to four others. This is the case for molecules of the intermediate dodecahedral $\{H_2O\}_{20}$ shell of **3a** (Figure 3, bottom right).

Structurally well-defined water shells can also be observed in the $\{Mo_{102}\} \equiv \{(Mo^{VI})Mo^{VI}_5\}_{12}\{Mo^{V}\}_{30}$-type cluster with a smaller cavity and containing acetate ligands.[16g,22] The much smaller cavity size only allows one to encapsulate a small $\{H_2O\}_{40}$ assembly consisting of two dodecahedral $\{H_2O\}_{20}$ shells, which corresponds practically to the two first shells in the cation-free $\{Mo_{132}\}$ capsule **3a**[16g] (see above). Generally speaking we can refer to a type of Aufbau principle (see for example, ref. [16g]) which is mainly based on the fact that the structures of water molecule assemblies are directed by the template influence of the five internal H_2O ligands coordinated to the five equivalent Mo atoms present in each of the 12 pentagonal $\{(Mo)Mo_5\}$-type units, like in **1a**, **2a**, and **3a**. This template effect leads especially to the generation of the $(H_2O)_{60} \equiv \{(H_2O)_5\}_{12}$ shell (see for instance ref. [25]). In the case of the presence of "larger" hydrophobic internal ligands such as acetates (not considered here), this template effect in the present type of capsule does not occur, as in the small $\{Mo_{102}\}$ cavity scenario.[22]

The influence of the internal bidentate ligands on the encapsulates can be nicely visualized by the following: Replacing, for instance, the 30 sulfate ligands in the corresponding $\{Mo_{132}\}$ Keplerate capsule by 30 small formate ligands—that is, getting **2a**—leads to the generation of 20 voids within the internal cavity shell surface (Figure 5, top) with the consequence that at these places an additional H_2O dodecahedron

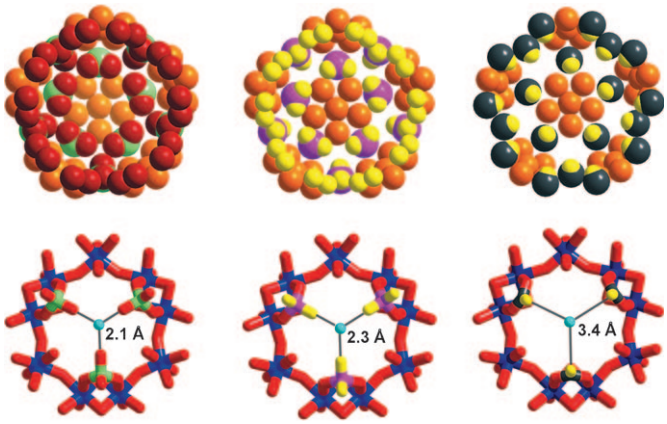

Figure 5. Demonstration of the influence of the replacement of SO_4^{2-} (left) by $PO_2H_2^-$[16g] (middle) and $HCOO^-$ ligands (right; change generates voids for 20 H_2O in **1a** like in the $PO_2H_2^-$ case) on the available space in the cavities, on the channel openings (bottom row), as well as on the internal shell structures (top row) of the related $\{Mo_{132}\}$ capsules. The pentagonal units with the different ligands (top row) as well as the related pores/channels (bottom row; in wireframe representation) in the corresponding clusters are shown in a view from the cluster center in direction of the C_5 and C_3 axes, respectively. The distances (Å) between the capsule center (turquoise sphere) of the narrowest channel area, and the O or H atoms of the ligands SO_4^{2-}, $PO_2H_2^-$, and $HCOO^-$ groups are given (color code for the top row: O (skeleton) orange, O (ligands) red, S green, P violet, H yellow, C black).

can be integrated with its 20 corners positioned at the C_3 axes.[16g] (The change to 30 hypophosphites instead has a similar effect.[16g]) But whereas in **1a** the related dodecahedral shell is completely filled it is only half-filled in the case of **2a** (reasons are given above).

One may ask general questions, such as: what is it like for molecules/ions to "house" inside a nanosized molecular container with respect to the interactions between them? In this context we can refer to two scenarios: 1) the interactions take place almost independently from the cavity-interior shell-functionalities (i.e. as in a nano-test-tube) or 2) they are influenced by the shell functionalities (see for instance ref. [24b]). In the present cases the latter scenario seems to be dominant due to an influence of the mentioned templates, that is, in agreement with the capsule symmetry.

"Water structures" are generally speaking typically affected by a surface/substrate which is lying not more than about 2 nm apart from them. In the context of the present work it is worthwhile mentioning that properties and activities(!) of interfacial water can be studied nicely on the surfaces of nanosized polyoxometalates, similar to the present ones, that is, also containing pentagonal units,[25] and that the exchange of H_2O ligands on mineral surfaces can be modeled by the present type of Keplerates.[26a] Note, the reactivity of water at mineral surfaces is important, for example, for sorption processes, the formation of soils, and the removal of CO_2 from the atmosphere (see, for example, ref. [26b]).

The following aspects might be interesting: Simulations have predicted that confined ice can have two symmetrically different phases which become deformed and indistinguishable when put under pressure.[27a] In this context a theoretician working in the field expected[27b] that one type of ice should easily transform into the other through collective motion of its hydrogen bonds, that "confined liquid water [···] will undergo similar structural rearrangements" and that this type of molecular mechanisms should also "[···] cause large changes to the network structure of water trapped in proteins or at membrane surfaces". (Reference to confined ice is in spite of the observed approximate icosahedral structures formally relevant here because the structures of **2** and **3** refer to measurements done at about 180 K.) The same author expected that these studies could help us "[···] to understand another intimate relationship—the relationship between water and life". (See in context the titles of two recently published reviews "Water as an active constituent in cell biology"[3b] and "Do we underestimate the importance of water in cell biology?".[4b]) In any case it is generally accepted that surface water and localized water clusters inside proteins—which are to some extent comparable to the present encapsulated water clusters with respect to their sizes—have a tremendous influence on the type of protein actions; see for example, references [4b,28].

The present type of studies based on a variety of capsule scenarios can give in the future more basic information about confined water and water electrolyte systems, about related (nano) fluid dynamics, and phase transitions if temperature-dependent investigations will be done as intended. (It is also intended in this context to synthesize a compound **3** type not containing **3b**.) This could lead to a better understanding of some related special topics of geo- and soil-sciences, as confined water plays, for example, a role in processes such as hydration and reactivity of mineral surfaces in natural environments (see for example, ref. [15,26]). Anyhow, we should accept that we are still a long way from a deeper understanding of the role of nearly ubiquitous "water" in all the mentioned scenarios.

Experimental Section

Synthesis of 1: HCOOH (60 mL, 10% in water) was added to a solution of $(NH_4)_{42}[(\{Mo\}Mo_5O_{21}\{H_2O\}_6)_{12}(Mo_2O_4\{CH_3COO\})_{30}]\cdot$ca. $[300\,H_2O+10\,CH_3COONH_4]$[16h] (3.00 g, 0.10 mmol) in water (55 mL). After the solution was stirred for 16 h at 80 °C and NH_4Cl (4.00 g, 74.80 mmol) was added, it was cooled to room temperature. The solution was left undisturbed for 10 days. The brownish rhombohedral precipitated crystals were collected by filtration over a glass frit, washed with ice cold water, ethanol, and diethyl ether, and dried in air over $CaCl_2$. Yield 2.3 g. After the compound had been dissolved at 60 °C for recrystallization in water (75 mL) containing NH_4Cl (3.00 g, 56.07 mmol), the solution was cooled to room temperature and left undisturbed for three days. The precipitated crystals of **1** were collected by filtration over a glass frit, washed with ice cold water, and dried over $CaCl_2$. Yield: 1.5 g; IR (KBr pellet): $\tilde{\nu}$ = 1620 (m, $\delta(H_2O)$) 1560 (m, ν_{as}(COO)), 1400 (m, $\delta([NH_4^+])/\nu_s$-(COO)), 1350 (w), 972 (m), 941 (w) (both ν(Mo=O)), 858 (w), 802 (s), 727 (s), 633 (w), 573 (s), 473 cm^{-1} (w); Raman (KBr dilution, λ_e = 1064 nm): $\tilde{\nu}$ = 945 (m, ν(Mo=O)), 878 (vs, O_{bri}-breathing), 850 (sh), 476 (w), 376 (m), 316 (w), 256 cm^{-1} (w) (preparation by Adrian–Raul Tomsa); elemental analysis calcd (%): C 1.31, H 3.46, N 2.14; found: C 1.3, H 3.2, N 2.2.

Synthesis of 2: A solution of **1** (0.50 g, 0.02 mmol) and formamidinium hydrochloride (0.38 g, 4.72 mmol) in water (20 mL) was heated to 65 °C for 15 min and then slowly cooled to room temperature. After six days the precipitated brown rhombohedral crystals of **2** were filtered over a glass frit, washed with ice cold water, ethanol, and diethyl ether, and dried over $CaCl_2$. Yield: 0.35 g; IR (KBr pellet): $\tilde{\nu}$ = 1718 (s, ν_{as}(C=N)), 1620 (m, $\delta(H_2O)$) 1560 (m, ν_{as}(COO)), 1387 (w), 1344 (w), 975 (m), 943 (w) (both (Mo=O)), 856 (w), 798 (s), 725 (s), 632 (w), 570 (s), 472 cm^{-1} (m); Raman (KBr dilution, λ_e = 1064 nm): $\tilde{\nu}$ = 946 (m, ν(Mo=O)), 879 (vs, O_{bri}-breathing), 850 (sh), 474 (w), 432 (w) 372 (s), 313 (m), 254 cm^{-1} (w) (preparation by Tamoghna Mitra); elemental analysis calcd (%): C, 3.19; H, 3.51; N, 4.54; found: C, 3.2; H, 3.2; N, 4.6.

Synthesis of 3:[23a] The compound was isolated from an aqueous solution of $(NH_4)_{42}[\{(Mo^{VI})Mo^{VI}_5O_{21}(H_2O)_6\}_{12}\{Mo^{V}_2O_4(H_2PO_2)\}_{30}]\cdot 300\,H_2O$ and $[(NH_2)_3C]_2SO_4$ after heating (details in ref. [16g]); elemental analysis calcd (%): C 2.23, H 3.11, N 7.80, P 1.92, S 1.32; found: C 2.5, H 2.9, N 7.2, P 1.9, S 1.1.

It should be mentioned that compounds containing formamidinium cations crystallize much better than those with guanidinium cations.

X-ray crystallographic data collection and refinement of the structure: Crystals of **1, 2**, and **3**[16f] were removed from the mother liquor and immediately cooled on a Bruker AXS SMART diffractometer (three-circle goniometer with 1 K CCD detector, $Mo_{K\alpha}$ radiation, graphite monochromator; hemisphere data collection in ω at 0.3° scan width in three runs with 606, 435, and 230 frames (φ = 0, 88 and 180°) at a detector distance of 5 cm). An empirical absorption correction using equivalent reflections was performed with the program SADABS 2.03. The structure was solved with the program SHELXS-97 and refined by using SHELXL-97 (SHELXS/L, SADABS from G. M. Sheldrick, University of Göttingen **1997/2001**; structure graphics with DIAMOND 2.1, DIAMOND 3.1 from K. Brandenburg, Crystal Impact GbR, **2001** and **2008**). CCDC-680565 (**1**) and CCDC-680566 (**2**) contain supplementary crystallographic data for

this paper. These data can be obtained free of charge from The Cambridge Crystallographic Data Centre via www.ccdc.cam.ac.uk/data_request/cif. Further details of the crystal structure determination of **3** may be obtained from the Fachinformationszentrum Karlsruhe, 76344 Eggenstein-Leopoldshafen, Germany (fax: (+49)7247–808–666; e-mail: crysdata@fiz-karlsruhe.de) on quoting the depository number CSD-412658.

Computational details: Classical molecular dynamics simulations were carried out on models of **1a**, **2a**, and **3a** in water as solvent. The geometry of the capsules was taken as in the corresponding single-crystal X-ray structures and kept frozen during the simulations. In the case of **1a**, the negative charge (−42) was neutralized with the corresponding number of sodium instead of ammonium cations. According to the disorder in the coordinates of **2** obtained crystallographically, the formamidinium cations in **2** were simulated by guanidinium cations for the sake of simplicity. For **3a** a fully substituted sulfate open capsule was considered instead of that with the mixed $H_2PO_2^-/SO_4^{2-}$ ligand system. The overall charge of −72 was neutralized with the corresponding number of hydrated Na^+ ions. Free motion of the cations and water molecules inside and outside the capsules was allowed under electrostatic and van der Waals interactions dictated by Lennard–Jones (LJ) potentials.

For the capsules, atomic charges were generated by using the QEq method[29] as implemented in the Materials Studio 4.0 Package. For water molecules, electrostatic and LJ parameters corresponded to those of the SPC/E model.[30] For the capsules, the LJ parameters were taken from previous work by our group.[31] For sulfur, oxygen, carbon, and hydrogen atoms the OPLS-AA parameters were used. The LJ parameters for monovalent cations were taken from Lee et al.[32] For the guanidinium cations, both the atomic charges and the LJ parameters were taken from the work of Weerasinghe et al.[33] Table S1 in the Supporting Information collects all the LJ parameters used.

All simulations were carried out using the DL_POLY2 program developed in the Daresbury Laboratory by W. Smith and T. R. Forester.[34] The trajectories of the systems along the simulations were analyzed in two ways. The radial distribution functions (RDFs) were computed and integrated with the Visual Molecular Dynamics 1.8.6. program, using a grid of 0.05 Å. Spatial distribution functions were computed in a grid with $231 \times 231 \times 231$ points, spaced 0.1 Å, based on a code written by the authors. A series of simulations using different conditions were considered, as indicated in Tables S2, S3, and S4 in the Supporting Information. Initially we considered capsule **3a** and checked whether the RDF profile was dependent on different factors or not. We found that the results were not dependent on the cation, that is, Na^+, nor on the temperature, nor on the presence or not of external solvent either. Therefore, simulations on capsule **2a** were run without external solvent, that is, in closed form. However, in this case it was necessary to reduce the temperature to obtain resolved peaks in the RDF profile.

Acknowledgement

A. M. gratefully acknowledges the financial support of the Deutsche Forschungsgemeinschaft (together with the National Science Foundation (USA)), the Fonds der Chemischen Industrie, the German–Israeli Foundation for Scientific Research & Development, the Volkswagenstiftung, and the European Union. P.M. thanks the Generalitat de Catalunya for a FI fellowship (2007FIC00043). We are indebted to the MEC of the Government of Spain (grants CTQ2005-0609-C02-02/BQU, CTQ2004-03346/PPQ and Consolider Ingenio 2010 CSD2006-0003), to the CIRIT of the Catalan Government (grants SGR01-00315, 2005SGR00715 and 2005SGR00104), and to the ICIQ Foundation for financial support. DL_POLY is a molecular dynamics simulation package written by W. Smith, T. R. Forester, and I. T. Todorov and has been obtained from CCLRC Daresbury Laboratory via the website http://www.ccp5.ac.uk/DL_POLY. The authors acknowledge the computer resources, technical expertise and assistance provided by the Barcelona Supercomputing Center—Centro Nacional de Supercomputación. We all thank Prof. V. Fedin, Dr. S. Roy, and E. Krickemeyer for their help in preliminary contributions regarding the syntheses of the compounds, which could only now for the first time be obtained in pure form with the well-defined water clusters.

[1] *Water in Confining Geometries* (Eds.: V. Buch, J. P. Devlin), Springer, Berlin, **2003**.

[2] a) D. A. Britz, A. N. Khlobystov, K. Porfyrakis, A. Ardavan, G. A. D. Briggs, *Chem. Commun.* **2005**, 37–39; b) J. Bai, J. Wang, X. C. Zeng, *Proc. Natl. Acad. Sci. USA* **2006**, *103*, 19664–19667, and references therein.

[3] a) P. Ball, *H_2O: A Biography of Water*, Weidenfeld & Nicolson, London, **1999**; b) P. Ball, *Chem. Rev.* **2008**, *108*, 74–108; c) P. Ball, *Cell. Mol. Biol.* **2001**, *47*, 717–720; d) P. Ball, *Nature* **2008**, *452*, 291–292.

[4] a) M. F. Chaplin, *Biophys. Chem.* **2000**, *83*, 211–221; b) M. F. Chaplin, *Nat. Rev. Mol. Cell Biol.* **2006**, *7*, 861–866.

[5] *Water—A comprehensive treatise, Vol. 1–7* (Ed.: F. Franks), Plenum, New York, **1972–1982**.

[6] R. Bukowski, K. Szalewicz, G. C. Groenenboom, A. van der Avoird, *Science* **2007**, *315*, 1249–1252.

[7] a) S. W. Benson, E. D. Siebert, *J. Am. Chem. Soc.* **1992**, *114*, 4269–4276; b) H. E. Stanley, S. V. Buldyrev, N. Giovambattista, E. La Nave, A. Scala, F. Sciortino, F. W. Starr, *Physica A.* **2002**, *306*, 230–242; c) F. N. Keutsch, R. J. Saykally, *Proc. Natl. Acad. Sci. USA* **2001**, *98*, 10533–10540; d) P. Wernet, D. Nordlund, U. Bergmann, M. Cavalleri, M. Odelius, H. Ogasawara, L. Å. Näslund, T. K. Hirsch, L. Ojamäe, P. Glatzel, L. G. M. Pettersson, A. Nilsson, *Science* **2004**, *304*, 995–999; e) W. H. Robertson, E. G. Diken, M. A. Johnson, *Science* **2003**, *301*, 320–321; f) Y. Zubavicus, M. Grunze, *Science* **2004**, *304*, 974–976; g) J. D. Smith, C. D. Cappa, B. M. Messer, R. C. Cohen, R. J. Saykally, *Science* **2005**, *308*, 793b; h) V. E. Bondybey, M. K. Beyer, *Int. Rev. Phys. Chem.* **2002**, *21*, 277–306 referring to the question "How many molecules make a solution?"; i) O. Mishima, H. E. Stanley, *Nature* **1998**, *396*, 329–335; j) M. Vedamuthu, S. Singh, G. W. Robinson, *J. Phys. Chem.* **1994**, *98*, 2222–2230; k) C. H. Cho, S. Singh, G. W. Robinson, *J. Chem. Phys.* **1997**, *107*, 7979–7988; l) G. W. Robinson, C. H. Cho, *Biophys. J.* **1999**, *77*, 3311–3318; m) R. Ludwig, *Angew. Chem.* **2001**, *113*, 1856–1876; *Angew. Chem. Int. Ed.* **2001**, *40*, 1808–1827.

[8] a) P. M. Wiggins, *Cell. Mol. Biol.* **2001**, *47*, 735–744; b) see also: P. M. Wiggins, *Microbiol. Rev.* **1990**, *54*, 432–449.

[9] a) P. Wiggins, *PLoS ONE* **2008**, *3*, 1–16; b) http://www.lsbu.ac.uk/water/protein.html (this is the most up to date collection of information about "water").

[10] M. Alcoutlabi, G. B. McKenna, *J. Phys. Condens. Matter* **2005**, *17*, R461-R524.

[11] a) R. Kurita, H. Tanaka, *Phys. Rev. Lett.* **2007**, *98*, 235701:1–4; b) C. Alba-Simionesco, B. Coasne, G. Dosseh, G. Dudziak, K. E. Gubbins, R. Radhakrishnan, M. Sliwinska-Bartkowiak, *J. Phys. Condens. Matter* **2006**, *18*, R15-R68.

[12] F. Mallamace, M. Broccio, C. Corsaro, A. Faraone, D. Majolino, V. Venuti, L. Liu, C.-Y. Mou, S.-H. Chen, *Proc. Natl. Acad. Sci. USA* **2007**, *104*, 424–428.

[13] M. Rovere, *J. Phys. Condens. Matter* **2004**, *16*, DOI: 10.1088/0953–8984/16/45/e01, and references therein.

[14] N. Floquet, J. P. Coulomb, N. Dufau, G. Andre, R. Kahn, *Adsorption* **2005**, *11*, 139–144.

[15] a) J. Wang, A. G. Kalinichev, R. J. Kirkpatrick, *J. Phys. Chem. B* **2005**, *109*, 14308–14313, and references therein; b) see also S.-H. Chen, L. Liu, E. Fratini, P. Baglioni, A. Faraone, E. Mamontov, *Proc. Natl. Acad. Sci. USA* **2006**, *103*, 9012–9016 where reference to high density (more fluid state) and low density (more solid state) water is made.

[16] a) A. Müller, S. Roy, *Coord. Chem. Rev.* **2003**, *245*, 153–166; b) A. Müller, S. Roy in *The Chemistry of Nanomaterials: Synthesis, Properties and Applications* (Eds.: C. N. R. Rao, A. Müller, A. K. Cheetham), Wiley-VCH, Weinheim, **2004**, pp. 452–475; c) See A. Merca, H. Bögge, M. Schmidtmann, Y. Zhou, E. T. K. Haupt, M. K. Sarker,

C. L. Hill, A. Müller, *Chem. Commun.* **2008**, 948–950 as well as E. T. K. Haupt, C. Wontorra, D. Rehder, A. Merca, A. Müller, *Chem. Eur. J.* **2008**, *14*, 8808–8811; d) A. Merca, E. T. K. Haupt, T. Mitra, H. Bögge, D. Rehder, A. Müller, *Chem. Eur. J.* **2007**, *13*, 7650–7658; e) A. M. Todea, A. Merca, H. Bögge, J. van Slageren, M. Dressel, L. Engelhardt, M. Luban, T. Glaser, M. Henry, A. Müller, *Angew. Chem.* **2007**, *119*, 6218–6222; *Angew. Chem. Int. Ed.* **2007**, *46*, 6106–6110; f) A. Müller, E. Krickemeyer, H. Bögge, M. Schmidtmann, S. Roy, A. Berkle, *Angew. Chem.* **2002**, *114*, 3756–3761; *Angew. Chem. Int. Ed.* **2002**, *41*, 3604–3609; g) A. Müller, E. Krickemeyer, H. Bögge, M. Schmidtmann, B. Botar, M. O. Talismanova, *Angew. Chem.* **2003**, *115*, 2131–2136; *Angew. Chem. Int. Ed.* **2003**, *42*, 2085–2090; h) A. Müller, S. K. Das, E. Krickemeyer, C. Kuhlmann, *Inorg. Synth.* (Ed.: J. R. Shapley), **2004**, *34*, 191–200; i) see for instance: A. Proust, R. Thouvenot, P. Gouzerh, *Chem. Commun.* **2008**, 1837–1852.

[17] a) O. Byl, J.-C. Liu, Y. Wang, W.-L. Yim, J. K. Johnson, J. T. Yates, Jr., *J. Am. Chem. Soc.* **2006**, *128*, 12090–12097; b) J. Shiomi, T. Kimura, S. Maruyama, *J. Phys. Chem. C* **2007**, *111*, 12188–12193; see also D. E. Moilanen, N. E. Levinger, D. B. Spry, M. D. Fayer, *J. Am. Chem. Soc.* **2007**, *129*, 14311–14318.

[18] D. E. Rosenfeld, C. A. Schmuttenmaer, *J. Phys. Chem. B* **2006**, *110*, 14304–14312.

[19] N. Jalarvo, H. N. Bordallo, N. Aliouane, M. A. Adams, J. Pieper, D. N. Argyriou *J. Phys. Chem. B* **2008**, *112*, 703–709.

[20] In this context it is important to note that this ligand exchange is based on some flexibility of the pores regarding partial opening which is one of the most important properties of the capsules. This is currently under investigation with NMR spectroscopy. An experimental/synthetic proof refers to the synthesis of the sulfate from the acetate $\{Mo_{132}\}$-type ball. At lower pH the acetate ligands get protonated while correspondingly leaving the capsule and sulfate ions are taken up: A. Müller, S. K. Das, S. Talismanov, S. Roy, E. Beckmann, H. Bögge, M. Schmidtmann, A. Merca, A. Berkle, L. Allouche, Y. Zhou, L. Zhang, *Angew. Chem.* **2003**, *115*, 5193–5198; *Angew. Chem. Int. Ed.* **2003**, *42*, 5039–5044.

[21] Compound **1** is different from the related earlier reported formate ligand based compound which contains extra lattice components NH_4^+ and $HCOO^-$ and another water structure: A. Müller, V. P. Fedin, C. Kuhlmann, H. Bögge, M. Schmidtmann, *Chem. Commun.* **1999**, 927–928.

[22] M. Henry, H. Bögge, E. Diemann, A. Müller, *J. Mol. Liq.* **2005**, *118*, 155–162.

[23] The overall formula of the compound containing **3a** and **3b** is: $(C(NH_2)_3)_{136}3[\{(C(NH_2)_3)_{20}+(H_2O)_{100}\}\subset\{(Mo)Mo_5O_{21}(H_2O)_6\}_{12}\text{-}\{Mo_2O_4(H_2PO_2)\}_{20}\{Mo_2O_4(SO_4)\}_{10}]\cdot[\{(C(NH_2)_3)_{20}+(H_2O)_{80}\}\subset\{(Mo)Mo_5O_{21}(H_2O)_6\}_{12}\{Mo_2O_4(H_2PO_2)\}_{12}\{Mo_2O_4(SO_4)\}_{18}]\cdot$ca. $400\,H_2O\equiv(C(NH_2)_3)_{136}\cdot(3\times\mathbf{3a})\cdot\mathbf{3b}\cdot$ca. $400\,H_2O\equiv\mathbf{3}$ (the formula corresponds to the cif file mentioned in ref. [16f], where **3b** was not referred to). In the related unit cell of the compound (space group $R\bar{3}m$[16f]) nine **3a** are on the $2/m$ and three **3b** on the $\bar{3}m$ sites (see the before published cif-file mentioned in the Experimental Section). But the structure of the water cluster is only nicely resolved in the capsules **3a**, while the capsules **3b** contain less water molecules. The earlier given formula of **3a**[16f] corresponds to a ligand ratio $H_2PO_2^-:SO_4^{2-}=20:10$. As the corresponding ligand ratio for **3b** is different, that is, 12:18, these capsules are more negatively charged, which leads to a larger attraction of cations. This is important as compound **3** was prepared from the NH_4^+ salt of the $\{Mo_{132}\}$-type cluster containing hypophosphite ligands[24a] with the consequence that even a very small number of (possibly) integrated cations, like one or two in the case of **3b** would therefore not allow the complete filling with water molecules, as observed for **3a**. As there is (still) a significant charge difference between **3a** and **3b** these appear as mentioned above on two different lattice sites. In this context it should also be noted that we have reached, in the special case of **3a** and **3b**, the limit of the exact determination of the number of (the two) different internal ligands present in the capsules (error limit ±2) not only because they appear crystallographically disordered but also because of the related analytical problem; **3** contains sulfur and phosphorus only in a very small amount (see Experimental Section). A problem also exists regarding the determination of a very small number of (possibly) encapsulated NH_4^+ ions in **3b**, as these would be—as usual—crystallographically disordered with H_2O molecules.

[24] a) A. Müller, S. Polarz, S. K. Das, E. Krickemeyer, H. Bögge, M. Schmidtmann, B. Hauptfleisch, *Angew. Chem.* **1999**, *111*, 3439–3443; *Angew. Chem. Int. Ed.* **1999**, *38*, 3241–3245; b) see for instance: A. Müller, L. Toma, H. Bögge, M. Henry, E. T. K. Haupt, A. Mix, F. L. Sousa, *Chem. Commun.* **2006**, 3396–3398.

[25] A. Oleinikova, H. Weingärtner, M. Chaplin, E. Diemann, H. Bögge, A. Müller, *ChemPhysChem* **2007**, *8*, 646–649.

[26] a) E. Balogh, A. M. Todea, A. Müller, W. H. Casey, *Inorg. Chem.* **2007**, *46*, 7087–7092; b) G. E. Brown Jr. , *Science* **2001**, *294*, 67–70; for geochemical aspects see also: W. H. Casey, J. R. Rustad, *Annu. Rev. Earth Planet. Sci.* **2007**, *35*, 21–46 and W. H. Casey, T. W. Swaddle, *Rev. Geophys.* **2003**, *41*, 1008.

[27] a) K. Koga, G. T. Gao, H. Tanaka, X. C. Zeng, *Nature* **2001**, *412*, 802–805I; b) I. Ohmine, *Nature* **2007**, *447*, 511.

[28] a) Regarding biological interfacial/confined water it is also important to look at the cytoplasm which contains up to 400 gL^{-1} macromolecules, that is, the cells are extremely "crowded". Therefore the macromolecules are only separated by about 1–2 nm, while the water hydrogen network is significantly disturbed causing coordination numbers of water molecules much lower (especially lower than four) than those in the bulk and those of the intermediate $\{H_2O\}_{20}$ dodecahedron in **3a** (green in Figure 1); see: D. S. Goodsell, *The Machinery of Life, S*pringer, New York, **1998** and ref. [3b]. b) Water plays also generally speaking a key role with regard to the interaction of the capsules with their environment. This refers to the cation transport through the inorganic membranes (E. T. K. Haupt, C. Wontorra, D. Rehder, A. Müller, *Chem. Commun.* **2005**, 3912–3914) and the type of interaction between the capsules' pores and positively charged plugs/guests present in the environment (see text).

[29] A. K. Rappé, W. A. Goddard III, *J. Phys. Chem.* **1991**, *95*, 3358–3363.

[30] H. J. C. Berendsen, J. R. Grigera, T. P. Straatsma, *J. Phys. Chem.* **1987**, *91*, 6269–6271.

[31] X. López, C. Nieto-Draghi, C. Bo, J. B. Avalos, J. M. Poblet, *J. Phys. Chem. A* **2005**, *109*, 1216–1222.

[32] S. H. Lee, J. C. Rasaiah, *J. Phys. Chem.* **1996**, *100*, 1420–1425.

[33] S. Weerasinghe, P. E. Smith, *J. Chem. Phys.* **2004**, *121*, 2180–2186.

[34] a) W. Smith, T. R. Forester, *J. Mol. Graph.* **1996**, *14*, 136–141; b) W. Smith, C. W. Yong, P. M. Rodger, *Mol. Simul. Mol. Sim.* **2002**, *28*, 385–471.

Received: August 4, 2008
Published online: January 7, 2009

